

NUMERICAL ANALYSIS OF CONVECTION–DIFFUSION WITH CHEMICAL REACTION BY COMBINED FINITE AND BOUNDARY ELEMENT METHODS

NAOTAKA OKAMOTO

Department of Applied Chemistry, Okayama University of Science, 1-1 Ridai-cho, Okayama 700, Japan

AND

MUTSUTO KAWAHARA

Department of Civil Engineering, Chuo University, 1-13-27 Kasuga, Bunkyo-ku, Tokyo 112, Japan

SUMMARY

A numerical method is presented to analyse a steady convection–diffusion problem with a first-order chemical reaction defined on an infinite region. The present method is based on the combined finite element and boundary element methods. For one- and two-dimensional examples in an infinite region the numerical results by the present method are in excellent agreement with the exact solutions. As a practical application, the simulation of the concentration distribution of the chemical oxygen demand at Kojima Bay is carried out.

KEY WORDS Convective diffusion Chemical reaction Finite element method Boundary element method
Combined method Coupling method COD

1. INTRODUCTION

It is important and valuable to solve convection–diffusion problems with a chemical reaction in the actual analysis such as waste water disposal, the red tide in the ocean, air pollution, etc. These are mainly characterized by their fields, which are to be analysed as their boundaries extend to infinity. The finite element method is one of the useful numerical tools for analysing such problems. It is, however, difficult to analyse a problem defined on an infinite region by use of finite element methods.¹ In numerical computations, boundary conditions must be introduced on the boundary of the area to be analysed. For these purposes, one of three types of boundary condition is imposed: (i) concentration, (ii) normal derivatives of concentration or (iii) normal component of flux. However, there are plenty of computational results indicating that these boundary conditions cannot result in a well-suited numerical concentration. This explains the actual problem observed with a field whose boundary extends to infinity. To overcome this difficulty, it is strictly necessary to introduce a scheme which can handle the infinite boundary condition. This boundary is referred to as the open boundary. There are two typical approaches to deal with the open boundary condition: (a) an artificial boundary condition is imposed or (b) an infinite element^{2,3} is attached. The first approach is preferable for us because the boundary element method satisfies unconditionally the infinite boundary condition by assuming that the problem is

linear. To obtain the artificial condition, the boundary element method is effectively used in this paper. We were not able to find any papers discussing the application of the approach to the steady convection–diffusion problem with a first-order chemical reaction defined on an infinite region. One of us proposed the boundary element method for the convection–diffusion problem with a first-order chemical reaction and obtained accurate numerical results in a previous paper.⁴ However, the boundary element method has difficulties in solving problems involving non-homogeneous fields because it is difficult to obtain the fundamental solution explicitly. If we appropriately combine the finite and boundary element methods, it is obvious that a method which covers the defects of both methods can be obtained for the convection–diffusion problem. This hybrid method is called the ‘combined method’ in this paper. A similar idea has been applied to several problems such as the electrostatic problem,⁵ wave propagation,⁶ etc.¹

In this paper we present a new numerical method to analyse steady convection–diffusion problems with or without a first-order chemical reaction defined on an infinite region. The present method is based on a combined method in which the boundary element method is applied to an unbounded region and the finite element method is applied to a bounded region. The validity of the present method is shown by three numerical examples. As a practical application, the concentration distribution of the COD (chemical oxygen demand) at Kojima Bay of Okayama prefecture in Japan is simulated and compared with the measured values.

2. BASIC EQUATION

This takes into consideration the steady convection–diffusion problem with a first-order chemical reaction on a two-dimensional infinite region Ω constructed from a finite element region $\Omega^{(F)}$ and a boundary element region $\Omega^{(B)}$ (Figure 1). The basic equation is expressed as

$$L[C_A] = -D\nabla^2 C_A + v \cdot \nabla C_A + kC_A = 0 \quad \text{in } \Omega = \Omega^{(F)} + \Omega^{(B)}, \quad (1)$$

where $L[\cdot]$, $C_A(P)$ and D denote the linear operator, the concentration of reactant A and the constant diffusivity respectively. The symbols ∇ , $v(P)$ and k denote the gradient operator, the velocity vector and the reaction rate constant respectively. $P(x, y)$ denotes a position and x, y denote the Cartesian co-ordinates. Let Γ_1 and Γ_2 be boundaries on which C_A and $\partial C_A/\partial n$ are defined respectively:

$$C_A(P) = \bar{C}_A(P) \quad \text{on } \Gamma_1, \quad (2a)$$

$$q_A(P) \equiv D\partial C_A/\partial n = \bar{q}_A(P) \quad \text{on } \Gamma_2, \quad (2b)$$

where $(\bar{\quad})$ denotes the prescribed function and n is the outer normal unit vector on the boundary.

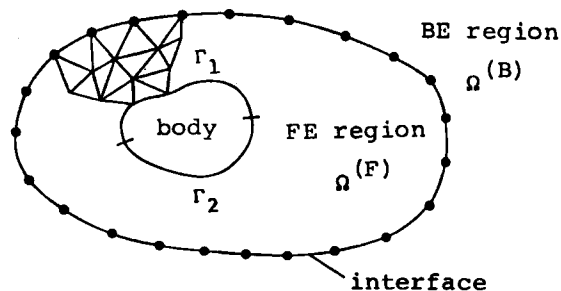


Figure 1. Bounded (finite elements) and unbounded regions

At infinity the boundary condition is expressed as

$$C_A(P) \rightarrow 0, \quad P \rightarrow \infty. \quad (3)$$

3. BOUNDARY ELEMENT METHOD

Green's second identity over Ω for equation (1) is expressed as

$$\int_{\Omega} (C_A^* L[C_A] - C_A L^*[C_A^*]) d\Omega = \int_{\Gamma_1} [(D\nabla C_A^*)C_A - C_A^*(D\nabla C_A) + vC_A^*C_A] \cdot n d\Gamma_1, \quad (4)$$

where $L^*[\cdot]$ and C_A^* denote the adjoint operator and the adjoint potential field to C_A respectively and Γ_1 denotes the interface between the finite and boundary element regions. The two-dimensional fundamental solution C^* should satisfy the following equation:

$$L^*[C^*] = -D\nabla^2 C^* - \nabla \cdot (vC^*) + kC^* = \delta(P_i - P), \quad (5)$$

where $\delta(\cdot)$, $P_i(x, y)$ and $P(\xi, \zeta)$ denote Dirac's delta function, an arbitrary source point and a reference point respectively. The two-dimensional fundamental solution $C^*(P_i, P)$ is given by

$$C^* = (1/2\pi D) \exp[-(v \cdot r)/2D] K_0^{(2)}(|\mu| |R|), \quad (6)$$

where

$$|R| = |P_i - P| = [(x - \xi)^2 + (y - \zeta)^2]^{1/2}, \quad (7a)$$

$$(v \cdot r) = v_x(x - \xi) + v_y(y - \zeta), \quad (7b)$$

$$\mu^2 = (|v_x|/2D)^2 + (|v_y|/2D)^2 + k/D \quad (7c)$$

and π and $K_0^{(2)}$ denote the ratio of the circumference of a circle to its diameter and a modified Bessel function of the second kind of order zero respectively. Equation (6) satisfies the infinite boundary condition (3). By choosing C^* instead of C_A^* in equation (4) and by applying equations (1) and (5) to equation (4), the following integral equation is obtained:

$$a(P_i)C_A(P_i) + \int_{\Gamma_1} D[\partial C^*(P_i, P)/\partial n]C_A(P) d\Gamma_1 + \int_{\Gamma_1} C^*(P_i, P)\{-D[\partial C_A(P)/\partial n] + v_n C_A(P)\} d\Gamma_1 = 0, \quad (8)$$

where $\partial/\partial n = n_x(\partial/\partial x) + n_y(\partial/\partial y)$ and $a(P_i)$ is the weight depending on the solid angle of Ω defined by

$$a(P_i) = \theta(P_i)/2\pi. \quad (9)$$

Here $\theta(P_i)$ is the external angle on the outer side of the bounded region if the boundary element is used in the external region. Assume that the interface is divided into M linear boundary elements ($j = 1, 2, \dots, M$). Then discretization of equation (9) gives

$$[H][U]_I^T = [G][Q]_I^T. \quad (10)$$

For simplicity, U , Q and I are used instead of C_A , q_A and Γ_1 respectively in matrix formulae. The (i, j) -components of $[H]$ and $[G]$ are respectively calculated as

$$H_{ij} = a(P_i)\delta_{ij} + \bar{H}_{ij}, \quad \bar{H}_{ij} = \int_{\Gamma_1} D[\partial C^*(P_i, P)/\partial n]F_j(P) d\Gamma, \quad (11a)$$

$$G_{ij} = \int_{\Gamma_i} C^*(P_i, P) F_j(P) d\Gamma, \quad (11b)$$

in which δ_{ij} denotes the Kronecker delta and $F_j(P)$ is a piecewise linear function. Since equation (1) includes the chemical reaction term, the conservation law for the calculation of the diagonal components of the matrix H cannot be satisfied. Namely, the diagonal component H_{ii} of the matrix H is

$$H_{ii} \neq - \sum_{j=1}^M H_{ij} \quad (i \neq j), \quad (12)$$

and the isoplethic concentration curve and Γ_i are not orthogonal to each other; therefore $\bar{H}_{ii} \neq 0$. Notice that H_{ii} must be calculated by equation (11).

4. COMBINATION OF THE FINITE AND BOUNDARY ELEMENT METHODS

The combined method of the finite and boundary element methods will now be described. To do this, the boundary elements are transformed into the equivalent finite elements.

Multiplying both sides of equation (10) by $[G]^{-1}$, the following equation is obtained:

$$[G]^{-1}[H][U^{(B)}]_I^T = [Q^{(B)}]_I^T, \quad (13)$$

where (B) denotes the boundary element region. In the bounded region, equation (1) is discretized by the finite element method using the linear element. Therefore the following equation is obtained:

$$\begin{bmatrix} [Y]_{RR} & [Y]_{RI} \\ [Y]_{IR} & [Y]_{II} \end{bmatrix} \begin{bmatrix} [U^{(F)}]_R^T \\ [U^{(F)}]_I^T \end{bmatrix} = \begin{bmatrix} [\bar{Q}_V^{(F)}]_R^T \\ [Q_V^{(F)}]_I^T \end{bmatrix}, \quad (14)$$

where the matrices are identified corresponding to the interface I and the bounded region R (note that the bounded region R is not involved with the interface) and in which (F) denotes the finite element region.

However, there is still a difficult problem, since Q is the flux at the node as opposed to Q_V which is the volume flux crossing the element on the interface for the combination of equations (13) and (14). Using the transformation matrix A , which can be considered as the continuity of the energy flow transmitted in the finite and boundary element regions, the following equation is obtained:⁷

$$[Q_V^{(F)}]_I^T = [A][Q^{(B)}]_I^T. \quad (15)$$

By the relation $[U^{(F)}]_I^T = [U^{(B)}]_I^T$ and from equations (13)–(15) the boundary elements can be transformed into the equivalent finite elements. Then the resulting global matrix is assembled as follows:

$$\begin{bmatrix} [Y]_{RR} & [Y]_{RI} \\ [Y]_{IR} & [Y]_{II} - [A][G]^{-1}[H] \end{bmatrix} \begin{bmatrix} [U]_R^T \\ [U]_I^T \end{bmatrix} = \begin{bmatrix} [\bar{Q}_V]_R^T \\ [0]_I^T \end{bmatrix}. \quad (16)$$

The transformation matrix is explained in the two-dimensional case. The relation of the continuity of the energy flow on each element of the interface Γ_{ie} is expressed in the following form:

$$\int_{\Gamma_{ie}} U^{(F)} Q_V^{(F)} d\Gamma = \int_{\Gamma_{ie}} U^{(B)} Q^{(B)} d\Gamma. \quad (17)$$

Using N_1 and N_2 as corresponding shape functions for the displacement of each node on the

interface, discretization can be carried out and leads to the following equation:

$$\begin{aligned}
 [U_1^{(F)} U_2^{(F)}] [Q_{V1}^{(F)} Q_{V2}^{(F)}]^T &= [U_1^{(F)} U_2^{(F)}] \left[\int_{\Gamma_{ie}} [N_1 N_2]^T Q_V^{(F)} d\Gamma \right] \\
 &= [U_1^{(B)} U_2^{(B)}] \left[\int_{\Gamma_{ie}} [N_1 N_2]^T [N_1 N_2] d\Gamma \right] [Q_1^{(B)} Q_2^{(B)}]^T.
 \end{aligned}
 \tag{18}$$

From the relation $[U_1^{(F)} U_2^{(F)}] = [U_1^{(B)} U_2^{(B)}]$ the following equations relating $Q_V^{(F)}$ and $Q^{(B)}$ are obtained:

$$Q_{V1}^{(F)} = \int_{\Gamma_{ie}} Q_V^{(F)} N_1 d\Gamma = l_i \left[\frac{1}{3} \frac{1}{6} \right] [Q_1^{(B)} Q_2^{(B)}]^T,
 \tag{19a}$$

$$Q_{V1}^{(F)} = \int_{\Gamma_{ie}} Q_V^{(F)} N_2 d\Gamma = l_i \left[\frac{1}{6} \frac{1}{3} \right] [Q_1^{(B)} Q_2^{(B)}]^T.
 \tag{19b}$$

Hence $[A]$ is given as

$$\begin{bmatrix}
 a_2(l_M + l_1) & a_1 l_1 & & & & & a_1 l_M \\
 a_1 l_1 & a_2(l_1 + l_2) & a_1 l_2 & & & & 0 \\
 & a_1 l_2 & a_2(l_2 + l_3) & a_1 l_3 & & & \\
 & & \dots & \dots & \dots & & \\
 & 0 & a_1 l_{i-1} & a_2(l_{i-1} + l_i) & a_1 l_i & & \\
 & & & \dots & \dots & & \\
 a_1 l_M & & & a_1 l_{M-1} & a_2(l_{M-1} + l_M) & &
 \end{bmatrix},
 \tag{20}$$

where $a_1 = \frac{1}{6}$, $a_2 = \frac{1}{3}$ and l_i is each element size with the finite and boundary elements combined.

On the other hand, in the one-dimensional case the transformation matrix $[A]$ is equal to $[1]$ and $Q^{(B)}$ is obtained analytically such that

$$Q^{(F)} = Q^{(B)} = D dC_A/dx = D\mu(1 - v_x/2D\mu)C_A, \quad \mu^2 = (|v_x|/2D)^2 + k/D.
 \tag{21}$$

5. NUMERICAL EXAMPLE

To examine the validity of the present method, three examples are shown. The following non-dimensional parameters are used: the non-dimensional concentration of the reactant, $\Phi = C_A/C_{A1}$, the non-dimensional co-ordinates $X = x/b$ and $Y = y/b$, the non-dimensional reaction rate constant $K = kb^2/D$ and the non-dimensional velocities $V_X = v_x b/D$ and $V_Y = v_y b/D$ ($Pe = V_X$ is called the Peclet number). Here C_{A1} is the characteristic concentration of the reactant and b is the characteristic length. The solutions are characterized by K and Pe .

Example 1 (one-dimensional case)

Here, in order to compare the numerical solution with the exact solution, the one-dimensional model is analysed. Therefore the one-dimensional fundamental solution for the boundary element method is used instead of equation (6):

$$C^* = (1/2\mu D) \exp[-v_x(x - \xi)/2D - |\mu||x - \xi|].
 \tag{22}$$

Figure 2 illustrates the finite element model for Example 1, where the finite element region (FE region) is discretized into 10 linear elements and the boundary element region (BE region) is combined at $X=1$. The boundary conditions are prescribed as

$$\text{BC1 } \Phi(0)=1, \quad \text{BC2 } \Phi(\infty)=0.$$

In Figure 3 the computed results of the combined method are compared with those of the finite element method for $K=2$. The solid lines show the exact solution. The boundary condition $d\Phi(1)/dx=0$ is applied for the finite element method. Figure 4 shows the relative errors of the numerical solutions by the combined method. It is seen that the numerical results of the combined method are in good agreement with the exact solution (i.e. the relative errors are less than 0.08%). The exact solution is described as follows:

$$\Phi = \exp\{(x/2)[V_X - (V_X^2 + 4K)^{1/2}]\}. \quad (23)$$

Example 2 (two-dimensional case)

Figure 5 shows the geometry of Example 2, where the finite element region ($0 \leq X, Y \leq 1$) is discretized into 200 triangular elements, the boundary element region is combined at $X=1$ and the flow direction is parallel to the X -co-ordinate. Example 2 is treated as the duct problem with an open outlet. The exact solution for this problem is not obtained. Instead of the exact solution,

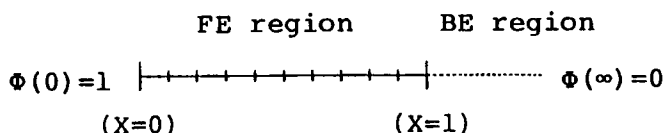


Figure 2. Numerical model for Example 1 (one-dimensional)

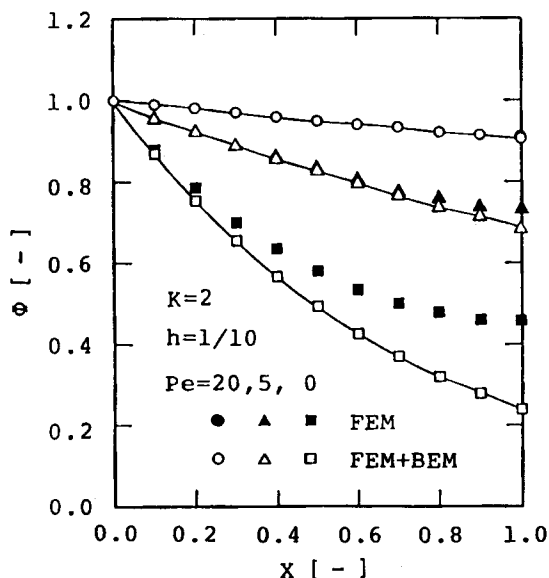


Figure 3. Numerical solutions for the one-dimensional problem (Example 1)

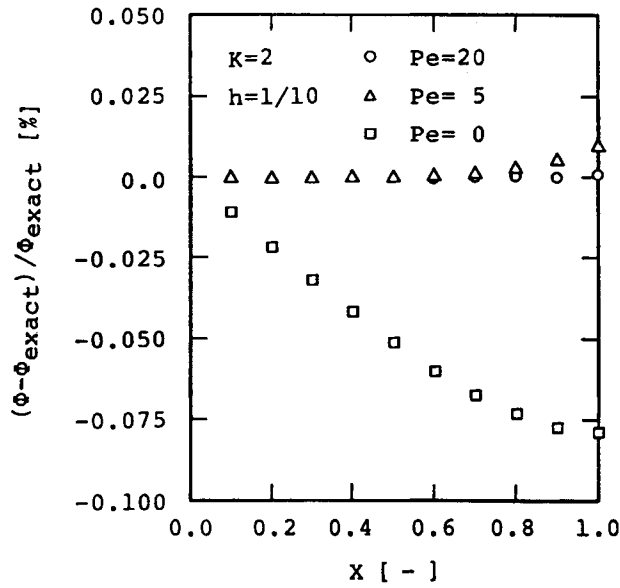


Figure 4. Relative errors of the numerical solutions for the one-dimensional problem (Example 1)

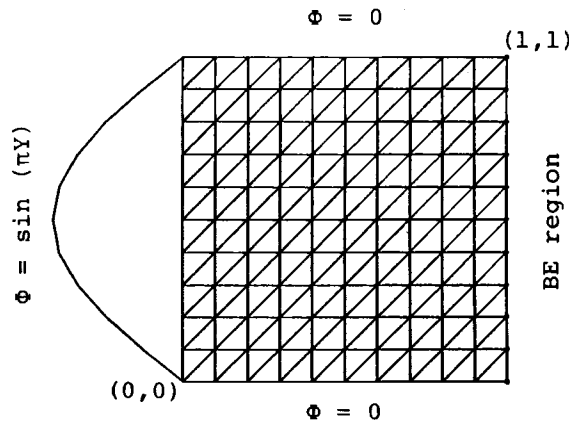


Figure 5. Numerical model for Example 2 (two-dimensional)

an analytical solution obtained for the following approximated boundary conditions is used for the comparative study. The exact solution on the line $(X, 0.5)$ approaches the analytical solution of equation (24) rapidly as the velocity increases.

$$\text{BC1 } \Phi(0, Y) = \sin(\pi Y), \quad \text{BC2 } \Phi(X, 0) = \Phi(X, 1) = 0, \quad \text{BC3 } \Phi(\infty, Y) = 0.$$

The numerical results are compared with the analytical solution on the line $(X, 0.5)$. The analytical solution is described as follows:

$$\Phi = [\sin(\pi Y)]^2 \exp\left\{\frac{X}{2} [V_x - (V_x + 4\pi^2 + 4K)^{1/2}]\right\}. \tag{24}$$

The boundary elements are used with linear elements; the components H_{ij} and G_{ij} ($i \neq j$) are evaluated numerically with the eight-point Gaussian quadrature rule, while the diagonal components H_{ii} and G_{ii} are evaluated with the 20-point Gaussian quadrature rule.

Figures 6(a) and 6(b) show the results of Example 2 for $K=0$ and 30 respectively along $Y=0.5$. The numerical results become well in agreement with the analytical solution as the velocity increases.

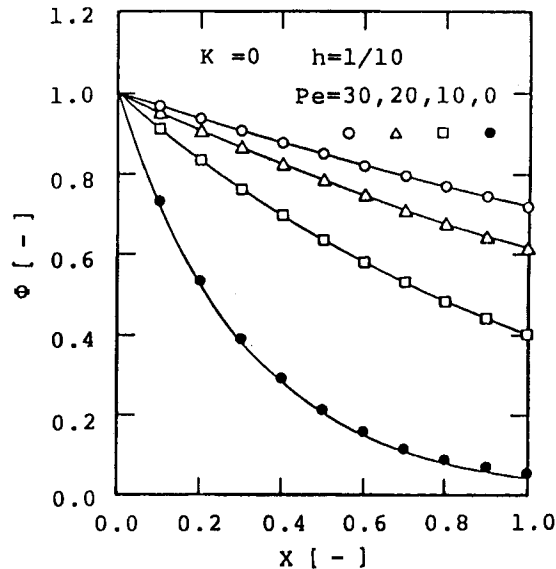


Figure 6(a). Numerical solutions for the two-dimensional problem (Example 2, $K=0$)

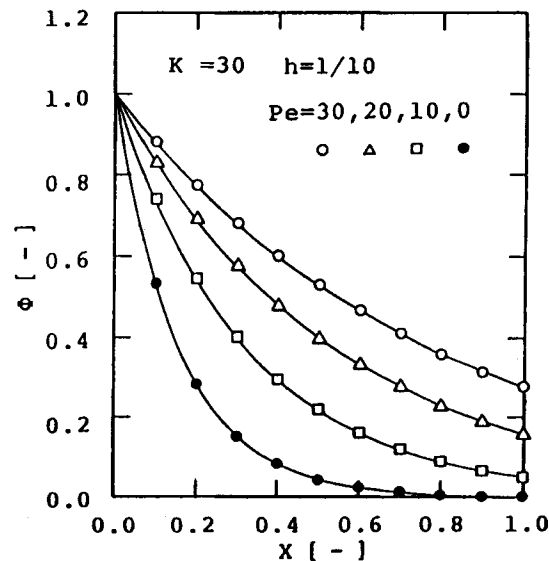


Figure 6(b). Numerical solutions for the two-dimensional problem (Example 2, $K=30$)

Example 3 (two-dimensional case)

Figure 7 illustrates Example 3, where the finite element region is discretized into 992 triangular elements and the boundary element region is combined around the finite element region. The reactant diffuses from the small square body to the infinite space. The velocity is assumed zero on the small square boundary and constant in the remaining area.

In the case of Example 3 the concentration distributions of the diffusion phenomenon can be computed in the infinite region. Also, a physically consistent concentration is obtained even in the region close to the interface. Figure 8 shows the concentration distributions with and without chemical reaction.

The analysis using the conventional finite element method of Example 3 is rather difficult because it is unclear how to set the boundary condition. The three conventional types of boundary condition cannot give reasonable results. For example, if $\partial C_A / \partial n = 0$ on the boundary is used, all the numerical results will be unitary in the case of a non-reaction system. If $N_A = (vC_A) \cdot n - D\partial C_A / \partial n = 0$ on the boundary is employed, the concentration near the outlet boundary is more than unity. Contrary to this, using the combined method, the analysis can be carried out naturally for the diffusion problem in the infinite region. The numerical result using the conventional finite element method is also shown in Figure 9 for comparison.

Note that the degree of freedom arising from the present method is equivalent to that in the linear equation arising from the finite element method for solving the problem defined on the truncated region. Therefore the CPU times for Example 3 are 106 s (on a FACOM380) for the finite element method and 114 s for the present method.

6. COD SIMULATION AT OKAYAMA BAY

Water which is polluted by actual drainage, etc. flows into Kojima Bay from the man-made Lake Kojima, Asahi River and Yoshii River. It is important to study the water pollution in order to improve the circumstances in the bay. In this section a simulation of the concentration distribution of the COD (chemical oxygen demand) at Kojima Bay is presented.

The flow distribution is calculated by the shallow water equation.⁸ Figure 10 shows the geometry of Kojima Bay, where the finite element region is discretized into 1698 triangular elements. The amounts of water inflow to Kojima Bay are 4996000 ton day⁻¹ from Asahi River,

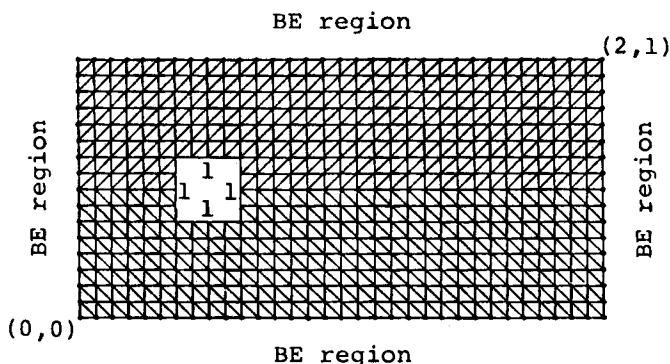


Figure 7. Numerical model for Example 3 (two-dimensional)

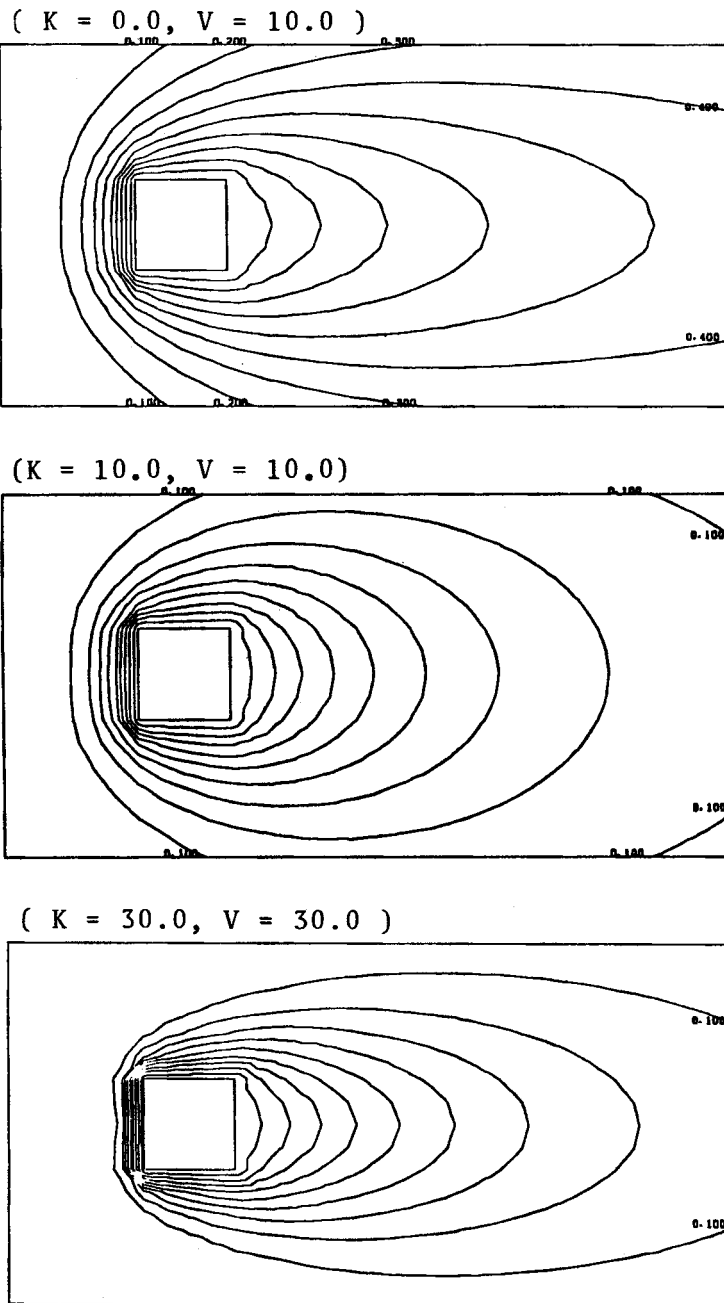


Figure 8. Concentration distributions (Example 3)

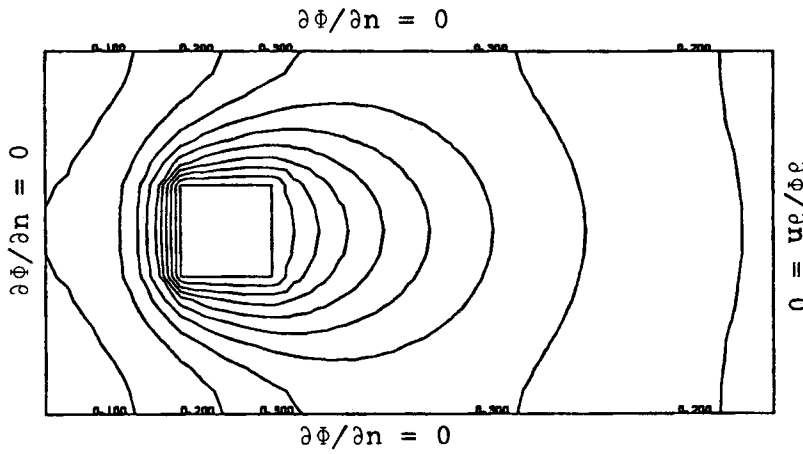


Figure 9. Concentration distribution using the conventional finite element method for $K=10$, $V=10$

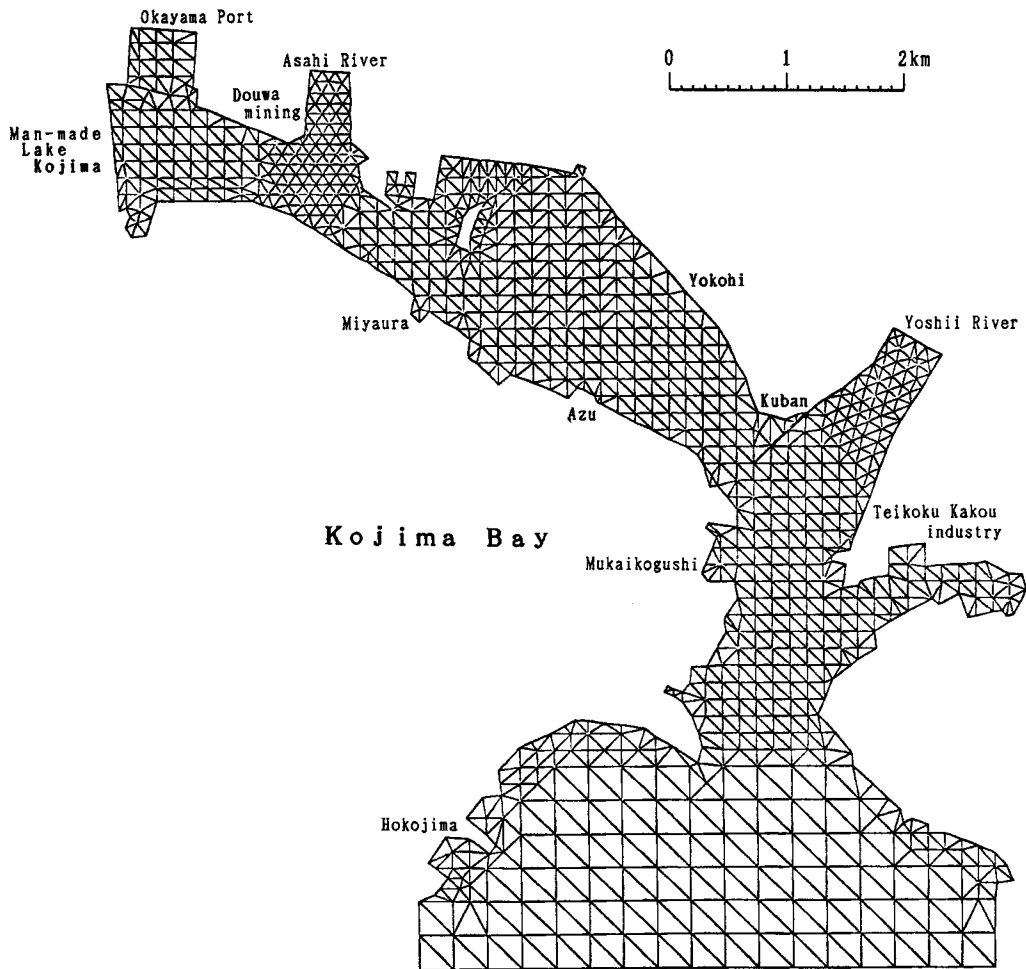


Figure 10. Finite element mesh of Kojima Bay

5006000 ton day⁻¹ from Yoshii River and 1200000 ton day⁻¹ from the floodgate of the man-made Lake Kojima. The depth of water is based on the data of Reference 9. The difference in water elevation between the floodgate in the man-made Lake Kojima and the entrance of Kojima Bay is set as 0.7 m and the water elevation is approximated linearly along the path from the lake to the bay. A slip condition is imposed on the wall boundary. The residual current velocity of the tide in Seto Inland Sea is estimated as 8.64 km day⁻¹ from west to east.¹⁰ The numerical method presented by Kawahara *et al.* is used with a lumping parameter of 0.8. Figure 11 shows the distribution of the residual current velocity.

The concentration distribution of the COD is analyzed. The data of the COD concentration of water from the river are based on the 1987 annual report.¹¹ The concentration gradient on the wall boundary is taken as zero ($\partial C_A / \partial n = 0$). The concentration is normalized by subtraction because the concentration in the infinite region is set to zero before the computation. After the computation is made, the concentration is denormalized by addition back to the original value.

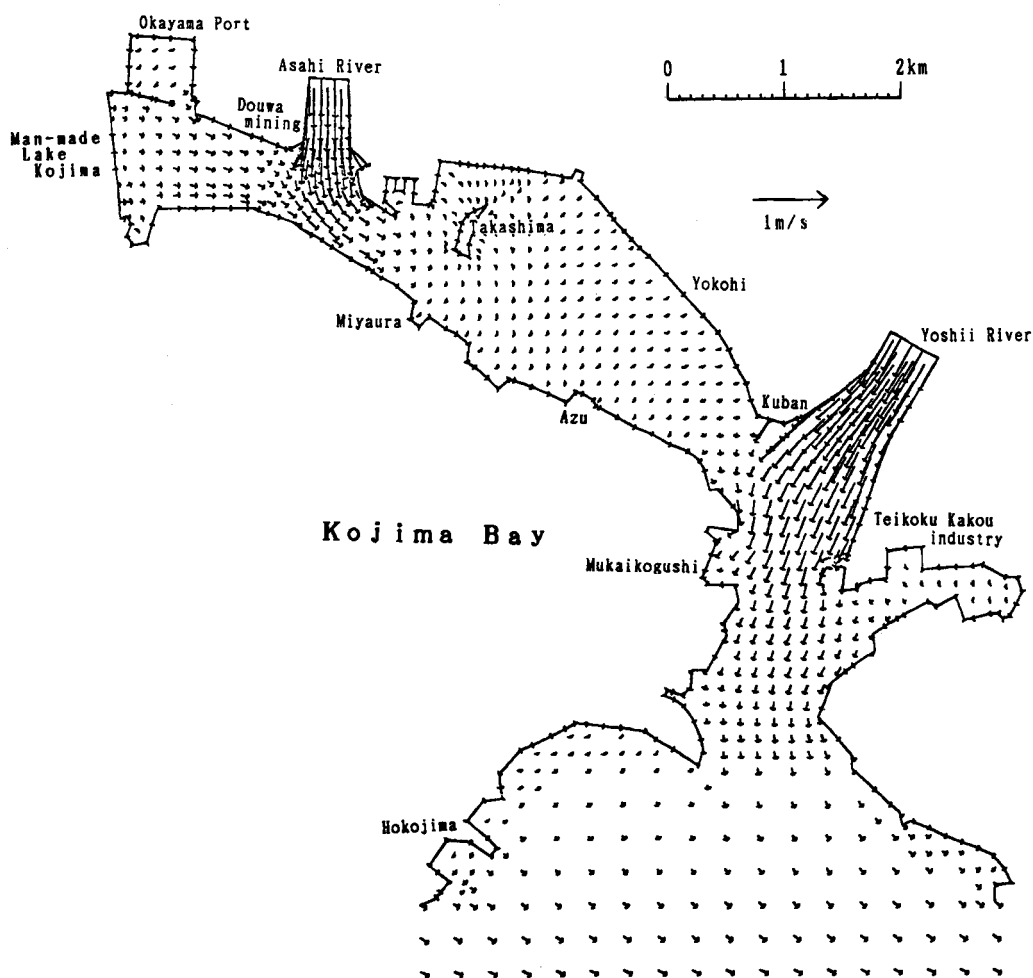


Figure 11. Residual current velocity at Kojima Bay

The COD concentration at Seto Inland Sea, regarded as a semi-infinite region, is estimated to be 1 mg l^{-1} by the 1987 annual report.¹¹ The COD concentration distribution is shown in Figure 12. The expressions with the unit 'mg/l', marked '⊙', are the values reported by the office of Okayama prefecture.¹¹ Judging from this comparison, it is seen that there is good agreement between the numerical results and the actual measurements. If we impose the Neumann condition on the entrance to the bay, diffusion to the external sea is not considered. However, diffusion to the external sea is actually an important factor in analysing the problem. In Figure 13 the numerical result using the finite element method is shown. The boundary condition at the entrance to the bay is set as $\partial C_A / \partial n = 0$. The concentration distribution in Figure 13 is different from that in Figure 12 around the entrance to the bay. The concentration distribution in Figure 13 does not correspond to the measured values. This fact shows that the combined method is superior to the conventional finite element method. Note that the values of the COD concentration and the volume of river water are determined from the annual averages.

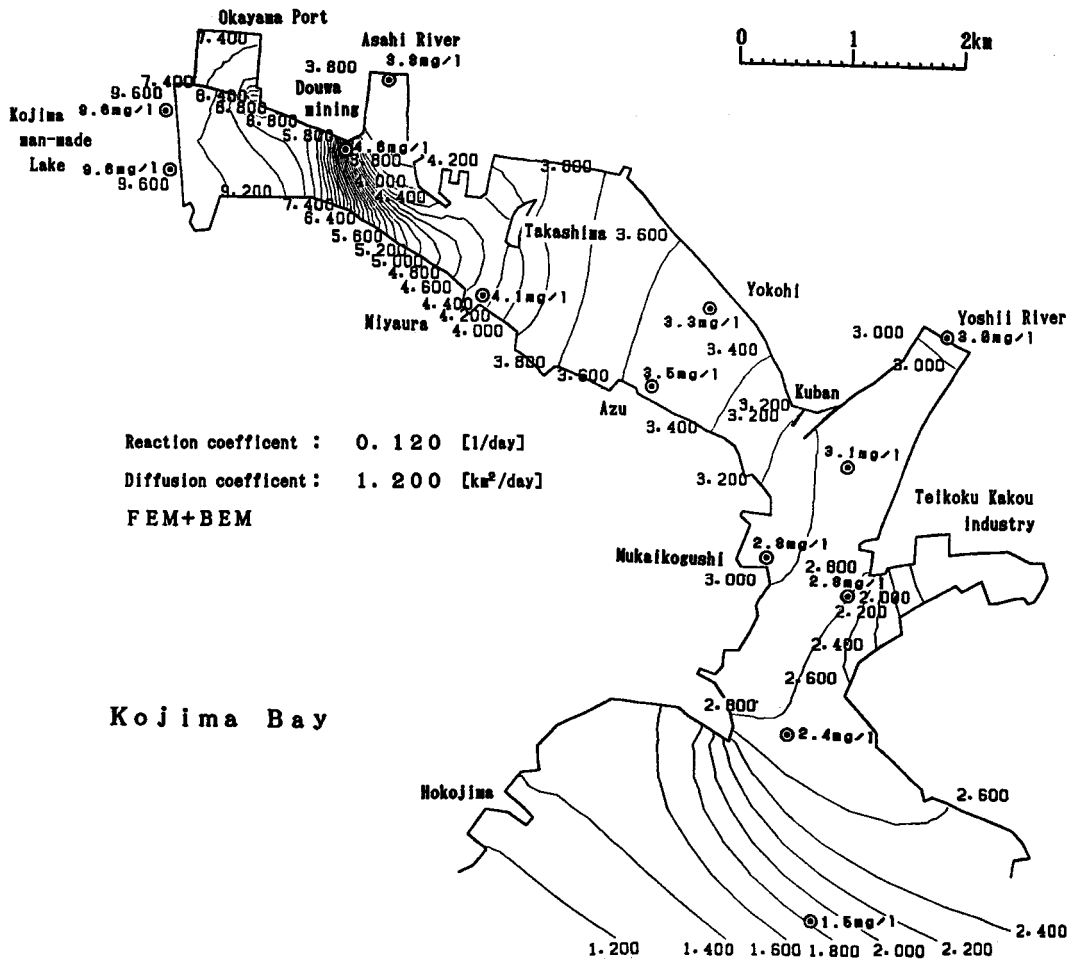


Figure 12. Computed and observed COD concentration distributions

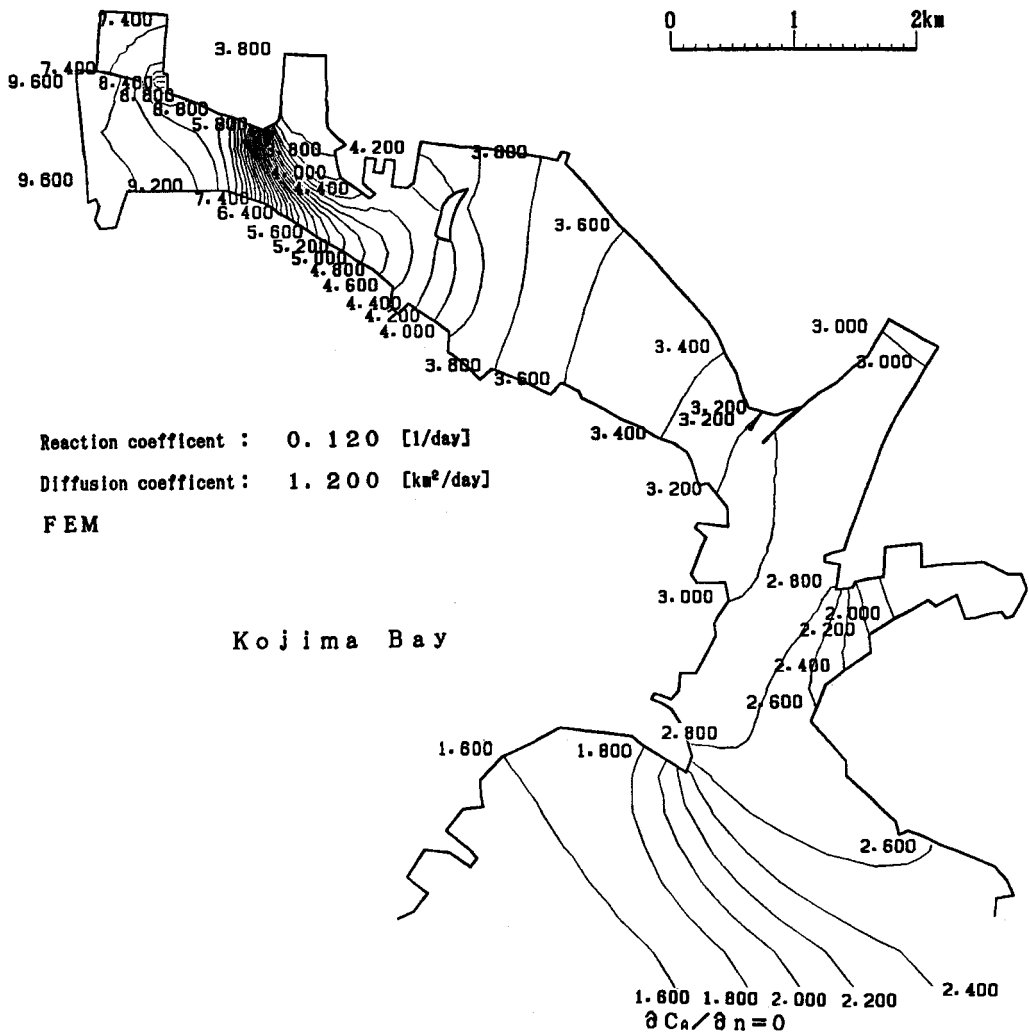


Figure 13. Computed COD concentration distribution using the conventional finite element method

7. CONCLUSIONS

A numerical method for solving convection-diffusion problems with a first-order chemical reaction defined on an infinite domain is presented in this paper. The present method is based on a combination of the finite and boundary element methods. By using the combined method, the infinity boundary condition can be satisfied unconditionally because of the property of the fundamental solution.

For Examples 1 and 2 we find that the numerical results by the present method are in good agreement with the exact solutions. In Example 3 we show the numerical result for the diffusion problem on the infinite region. This is difficult to obtain using the conventional method. The present method has been applied successfully to the concentration diffusion analysis of Kojima Bay. It is concluded from the numerical examples that the present method is remarkably superior to the conventional method.

REFERENCES

1. O. C. Zienkiewicz, *The Finite Element Method*, McGraw-Hill, London, 3rd edn, 1977.
2. H. Hara, O. C. Zienkiewicz and P. Bettess, 'Application of finite elements to determination of wave effects on offshore structures', *Proc. 2nd Int. Conf. on Behaviour of Off-Shore Structures*, held at Imperial College, London, Secretariat provided by BHRA Fluid Engineering, Cranfield Bedford, England, 1979, pp. 383-390.
3. P. Bettess, 'Infinite elements', *Int. j. numer. methods eng.*, **11**, 53-64 (1977).
4. N. Okamoto, 'Analysis of convection-diffusion problem with first-order chemical reaction by boundary element method', *Int. j. numer. methods fluids*, **8**, 55-64 (1988).
5. O. C. Zienkiewicz, D. W. Kelly and P. Bettess, 'The coupling of the finite element method and boundary solution procedures', *Int. j. numer. methods eng.*, **11**, 355-374 (1977).
6. M. Kawahara and K. Kashiwama, 'Boundary type finite element method for surface wave motion based on trigonometric function interpolation', *Int. j. numer. methods eng.*, **21**, 1833-1852 (1985).
7. Y. Kagawa, *Kairyōiki mondai no tameno yūgen kyōkai yōsōhō*, Saiensusha, Tokyo, 1983, pp. 135-165 (in Japanese).
8. M. Kawahara, H. Hirano, K. Tsubota and K. Inagaki, 'Selective lumping finite element method for shallow water flow', *Int. j. numer. methods fluids*, **2**, 89-112 (1982).
9. Maritime Safety Agency, *Nippon Seto naikai Okayama suidō No. 155*, 1987.
10. Okayama prefecture, *Okayamakou kouwan keikakusyo*, 1986 (in Japanese).
11. Okayama prefecture, *Kokyo yōsuiiki suisitu sokutei kekka*, October 1987 (in Japanese).